Applied Physics Letters ARTICLE pubs.aip.org/aip/apl

Defects and oxygen impurities in ferroelectric wurtzite $Al_{1-x}Sc_xN$ alloys

Cite as: Appl. Phys. Lett. **125**, 022901 (2024); doi: 10.1063/5.0211892
Submitted: 2 April 2024 · Accepted: 21 June 2024 ·
Published Online: 9 July 2024

Cheng-Wei Lee,[1] Naseem Ud Din,[1] Geoff L. Brennecka,[1] and Prashun Gorai[1,2,a)]

AFFILIATIONS

[1]Colorado School of Mines, Golden, Colorado 80401, USA
[2]Rensselaer Polytechnic Institute, Troy, New York 12180, USA

[a)]Author to whom correspondence should be addressed: pgorai@mines.edu

ABSTRACT

III-nitrides and related alloys are widely used for optoelectronics and as acoustic resonators. Ferroelectric wurtzite nitrides are of particular interest because of their potential for direct integration with Si and wide bandgap semiconductors and unique polarization switching characteristics; such interest has taken off since the first report of ferroelectric $Al_{1-x}Sc_xN$ alloys. However, the coercive fields needed to switch polarization are on the order of MV/cm, which are 1–2 orders of magnitude larger than oxide perovskite ferroelectrics. Atomic-scale point defects are known to impact the dielectric properties, including breakdown fields and leakage currents, as well as ferroelectric switching. However, very little is known about the native defects and impurities in $Al_{1-x}Sc_xN$ and their effect on the dielectric and ferroelectric properties. In this study, we use first-principles calculations to determine the formation energetics of native defects and unintentional oxygen incorporation and their effects on the polarization switching barriers in $Al_{1-x}Sc_xN$ alloys. We find that nitrogen vacancies are the dominant native defects, and unintentional oxygen incorporation on the nitrogen site is present in high concentrations. They introduce multiple mid-gap states that can lead to premature dielectric breakdown and increased temperature-activated leakage currents in ferroelectrics. We also find that nitrogen vacancy and substitutional oxygen reduce the switching barrier in $Al_{1-x}Sc_xN$ at low Sc compositions. The effect is minimal or even negative (increases barrier) at higher Sc compositions. Unintentional defects are generally considered to adversely affect ferroelectric properties, but our findings reveal that controlled introduction of point defects by tuning synthesis conditions can instead benefit polarization switching in ferroelectric $Al_{1-x}Sc_xN$ at certain compositions.

It has been long known that wurtzite nitrides, including AlN and GaN, have large spontaneous polarization $> 100\ \mu C/cm^2$, but the electric fields needed to reverse the polarization (for ferroelectricity) are larger than the dielectric breakdown fields.[1,2] There has been a resurgence of interest in wurtzite and wurtzite-type ferroelectrics since the unexpected demonstration of robust polarization switching in $Al_{1-x}Sc_xN$ alloys.[3] Polarization switching has now been demonstrated in other solid solutions, including $Al_{1-x}B_xN$, $Al_{1-x}Y_xN$, $Ga_{1-x}Sc_xN$, and $Zn_{1-x}Mg_xO$.[4–7] New binary and multinary compounds have also been proposed for wurtzite-type ferroelectrics.[2,8,9]

There are both scientific and technological reasons to be excited about this new class of ferroelectric materials—from the fundamentally new physical mechanisms driving polarization switching[10–12] to the possibility of direct integration with commercial microelectronics enabling in-memory computing, high-density data storage, and electro-optics.[13,14] Yet, there are several challenges facing the deployment of wurtzite-type ferroelectric devices, among which lowering of the switching barrier (i.e., coercive field) while remaining highly insulating is the most pressing. Empirically, coercive field reduction has so far been achieved via strain engineering,[3,15] increased operating temperature,[16] and with higher alloying substitutions. However, significant experimental data and phenomenological modeling both suggest that these approaches have limited impact.[17] A more rational approach to lowering coercive fields while also maintaining high breakdown fields will require an understanding of the atomic-scale mechanisms.

There is ample evidence on the influence of defects on the ferroelectric behavior in oxide perovskites[18] and emerging materials, such as HfO_2.[19] However, the defect makeup and their effects on the ferroelectric properties of wurtzite-type compounds and solid solutions remain unclear. We know from fundamental physics that defects, including atomic-scale point defects to extended defects, such as stacking faults and dislocations, are likely to affect ferroelectric properties. Charged shallow defects create free electronic carriers (electrons and holes) that contribute to leakage current; in contrast, deep defects

localize the electronic carriers and minimize the increase in the leakage current but may lead to the premature dielectric breakdown. Point defects are also known to locally modify the polarization switching and affect domain wall motion by pinning in oxide ferroelectrics,[20] but their role(s) on wurtzite polarization reversal are unknown.

Our current understanding of the defect physics in wurtzite-type materials is mostly based on binary wurtzite compounds, e.g., GaN and AlN.[21–24] For isostructural alloys between wurtzite compounds, linear interpolation between parent compounds is generally assumed.[23] However, for heterostructural alloys, such as $Al_{1-x}Sc_xN$ (wurtzite AlN and rock salt ScN), the validity of such interpolation is unclear. An experimental study has proposed nitrogen vacancies as a possible origin of leakage current in $Al_{1-x}Sc_xN$ thin films.[25] A computational study probed the formation thermodynamics of nitrogen vacancy (V_N), which qualitatively supports its contribution to the leakage current in $Al_{1-x}Sc_xN$.[26] However, that study suffers from several technical issues in addition to considering only single $Al_{1-x}Sc_xN$ composition ($x = 0.25$). The study did not consider cation vacancies, limits on the elemental chemical potentials set by phase stability, bandgap correction, or quantify the defect or electronic carrier concentrations. These details are critical for accurate quantitative predictions.

Additionally, while the majority of studies do not explicitly address oxygen incorporation, it is an experimental reality that all samples have a non-zero amount of oxygen incorporation. Oxygen substituting on the nitrogen site (O_N) is a known donor defect in III-nitrides, and a DX center in some cases, e.g., in AlN and related alloys.[22,23,27] Therefore, quantifying O_N and understanding its behavior are critical since shallow donors generate free electrons and contribute to increased leakage currents while deep defects can cause premature dielectric breakdown. Here, we use first-principles defect calculations to determine the formation thermodynamics of native defects and unintentional oxygen impurity incorporation in $Al_{1-x}Sc_xN$ alloys ($x = 0 - 0.333$). Specifically, we want to answer: (1) Which defects are present in high concentration and under what growth conditions? (2) Are deep defects present and what are their energetic location? (3) What is the level of unintentional oxygen incorporation—common in many nitrides and nitride-based alloys? and (4) What are the associated electronic carrier concentrations?

To address these questions, we used our methodology for modeling defects in alloys.[28,29] In this approach, we predict an *effective* defect formation energy, which approximately accounts for the variations in the formation energy in different local environments in the alloy. The effective formation energy can be thought of as a statistical average formation energy across the different sites in the alloy. Total energy calculations and structural relaxations were performed with density functional theory, as implemented in Vienna Ab Initio Software Package. Details of the computational methodology are provided in the supplementary material. We calculated the formation energetics of native defects and oxygen incorporation in $Al_{1-x}Sc_xN$ with varying Sc content in the range $x = 0$–0.333, where the wurtzite phase is stable and includes the range of x where ferroelectric switching is experimentally observed. Specifically, we examined the defect properties at $x = 0.042$, 0.125, 0.250, and 0.333, all in the wurtzite phase.

The computed effective formation energy ($\Delta E_{D,q}$) of native defects and substitutional oxygen (O_N) are shown in Fig. 1 for $x = 0.333$. Here, we focus on $Al_{0.667}Sc_{0.333}N$, i.e., $x = 0.333$, only because the qualitative trends across different compositions are similar and compositions with $x > 0.3$ are most relevant for ferroelectric studies. $\Delta E_{D,q}$ is computed for Al vacancy (V_{Al}), Sc vacancy (V_{Sc}), and nitrogen vacancy (V_N) defects. We did not consider metal/N antisite defects and interstitials because of their high formation energy in AlN.[24] The equilibrium Fermi energy ($E_{F,eq}$) in each case is calculated self-consistently by solving for charge neutrality at 1000 K. Calculated $\Delta E_{D,q}$ at $x = 0.042$, 0.125, and 0.250 are presented in Figs. S4–S6.

Under N-rich growth conditions [Fig. 1(a)], V_{Al}, V_{Sc}, and V_N form in low and comparable concentrations due to their very high formation energies; V_N concentration is $\sim 10^4\,cm^{-3}$ at 1000 K [Fig. 2(a)]. In contrast, we find that V_N is the dominant defect under the most N-poor growth conditions [Fig. 1(a)], with equilibrium concentration exceeding $10^{16}\,cm^{-3}$. Both metal and anion vacancies exhibit amphoteric behavior, i.e., capable of acting as donor *and* acceptor depending on E_F. High concentrations of V_N and its amphoteric nature in AlN, GaN, and other III-nitrides are well documented.[22,29,30] Therefore, it is unsurprising to find that V_N is the dominant defect, especially under N-poor growth conditions. Our calculations suggest that growth under more N-rich conditions will result in less defective $Al_{1-x}Sc_xN$, which is generally desired to sustain larger dielectric breakdown fields, reduced leakage currents, and potentially more robust polarization switching.

Thin films of III-nitrides and related alloys commonly incorporate oxygen as an impurity.[31–33] The unintentional oxygen incorporation during growth or ambient exposure has adverse effects on the structural and optoelectronic properties of these materials.[22,33] Specifically, oxygen substituting on the nitrogen site leads to the creation of donor defect states that have been associated with temperature-activated leakage currents in AlN.[34] Given the possibility of substantial oxygen incorporation in $Al_{1-x}Sc_xN$ alloys, it is crucial to quantify the level of oxygen incorporation and determine if they introduce deep defect states. We calculated $\Delta E_{D,q}$ of oxygen substitution on the nitrogen site (O_N) at each of the four compositions discussed above. Figures 1(c) and 1(d) show the defect energetics of O_N in $Al_{0.667}Sc_{0.333}N$, while the defect energetics for $x = 0.042$, 0.125, and 0.250 are shown in Figs. S4–S6, respectively. Unlike V_N, O_N is the dominant defect (high concentration) under both N-rich and most N-poor growth conditions, suggesting high levels of unintentional O incorporation unless oxygen exposure during growth is carefully eliminated. Similar trends are observed at other compositions (Figs. S4–S6).

We find that both V_N and O_N introduce multiple deep mid-gap states in $Al_{1-x}Sc_xN$. The charge transition levels (CTLs) of V_N are shown in Fig. 3 at various alloy compositions. The CTLs are referenced to the valence band maxima (VBM). The bandgap is calculated using the GW method (see the supplementary material for details), which shows a monotonic decrease with increasing x since ScN has a significantly smaller bandgap (~ 1 eV)[35] relative to AlN (calculated 6.1 eV). O_N is a known DX center in AlN.[23] A DX center is a deep defect that forms when a donor defect like O_N^{+1} captures two electrons and undergoes a large local structural distortion to stabilize an acceptor state like O_N^{-1}. As a result, a key feature of a DX center is displacement of the O atom from the ideal N site. DX centers are commonly observed in zinc blende and wurtzite compounds.[36] For $Al_{1-x}Sc_xN$ alloys, we find O_N^{-1} has the characteristics of a DX center (e.g., see structures in Fig. S7 for $x = 0.333$). Both deep defects are undesirable for optoelectronics because they act as carrier recombination centers. In ferroelectrics, deep defects can mediate premature dielectric breakdown before

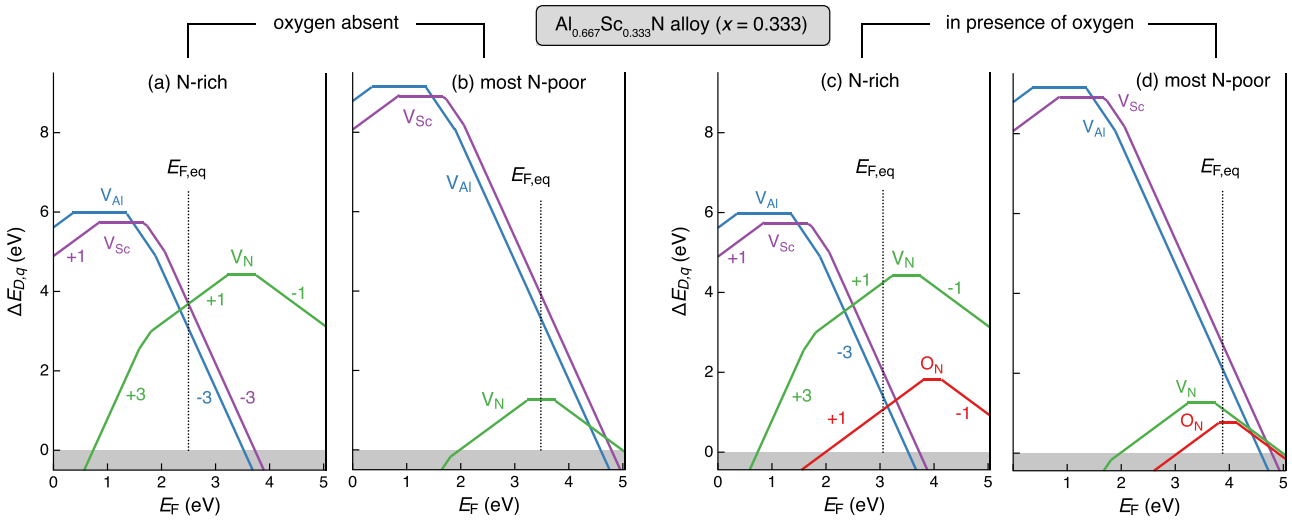

FIG. 1. Defect formation energy ($\Delta E_{D,q}$) as a function of the Fermi energy (E_F) in $Al_{0.667}Sc_{0.333}N$ alloy when oxygen is absent [(a) and (b)] and present [(c) and (d)]. The equilibrium Fermi energy ($E_{F,eq}$) is calculated at $T = 1000$ K. Defect energetics are calculated under N-rich [(a) and (c)] and most N-poor growth conditions [(b) and (d)] corresponding to the chemical potentials at vertices V4 and V1 of the phase stability region in Table S5, respectively.

polarization switching but can be beneficial for electronic carrier trapping that suppresses leakage currents.

The breakdown field of an insulator critically depends on the bandgap of the material. Considering the importance of the breakdown field for polarization switching, we semi-quantitatively estimate the effect of Sc composition (x) on the intrinsic breakdown field (E_b, in MV/m) of $Al_{1-x}Sc_xN$. We used a phenomenological model[37] to estimate E_b as follows:

$$E_b = 24.442 \exp\left(0.315\sqrt{E_g \omega_{max}}\right), \quad (1)$$

which depends on the electronic bandgap (E_g, in eV) and the maximum optical phonon frequency (ω_{max}, in THz) at the Γ point of the Brillouin zone. E_g of the alloys calculated with the GW method (Fig. 3) monotonically decreases with x. Direct calculation of ω_{max} for alloys is computationally expensive, but we can draw trends based on ω_{max} of pure wurtzite-AlN (~26.98 THz) and rock salt-ScN (~19.49–20.99 THz). We expect a decrease in ω_{max} with increasing x, consistent with the increased softening of $Al_{1-x}Sc_xN$. With pure AlN ($E_g = 6.11$ eV) as the reference and no change in ω_{max}, E_b will decrease by 4%, 9%, 18%, and 20% at $x = 0.042$, 0.125, 0.250, and 0.333, respectively. The decrease in ω_{max} with x will further exacerbate the decrease in E_b.

Charged defects introduce electronic carriers (free or bound) that contribute to leakage currents. We estimate the net carrier concentrations self-consistently by solving for charge neutrality. The net carrier concentration computed as $|n_h - n_e|$ is shown in Fig. 2(c), corresponding to the defect energetics in Figs. 1(a) and 1(b), where no

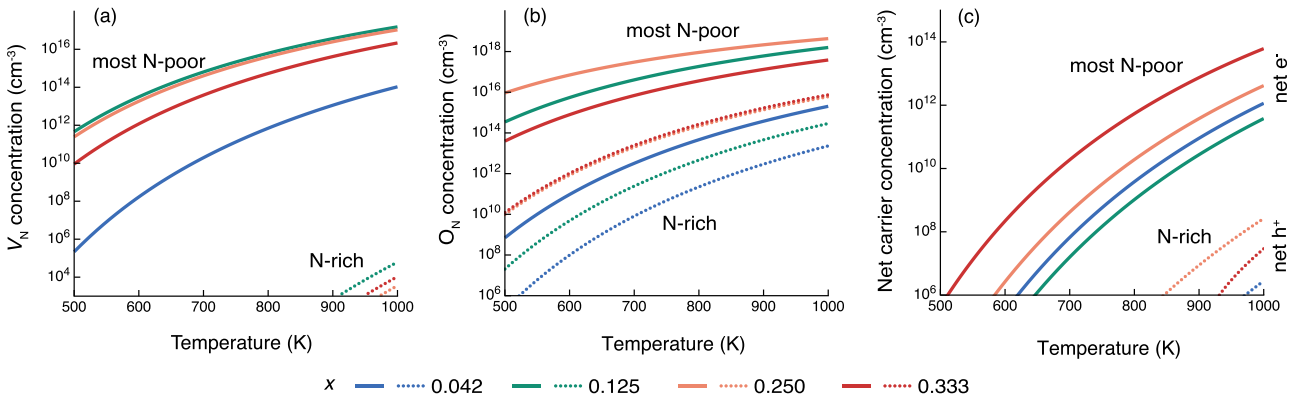

FIG. 2. Net carrier concentration in $Al_{1-x}Sc_xN$ for $x = 0.042$, 0.125, 0.250, and 0.333 under N-rich and most N-poor growth conditions. (a) Nitrogen vacancy (V_N) concentrations under most N-poor growth conditions (solid lines). Under N-rich conditions (dotted lines), V_N concentrations are lower $<10^6$ cm^{-3}. (b) Substitutional O_N concentrations under most N-poor (solid) and N-rich (dotted) growth conditions. (c) Net carrier concentration is $|n_e - n_h|$, where n_e and n_h are electron and hole concentrations, respectively. Under most N-poor conditions, $n_e > n_h$ while $n_h > n_e$ under N-rich conditions.

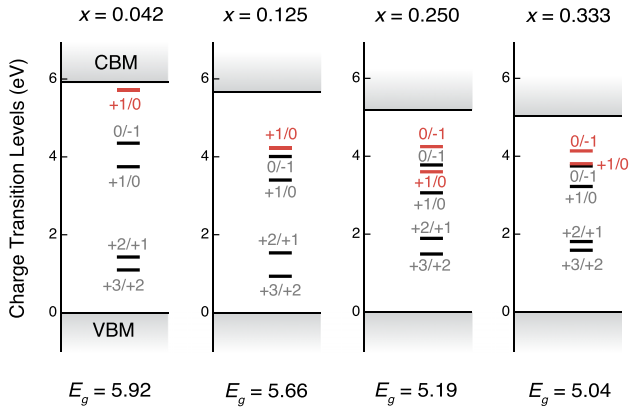

FIG. 3. Charge transition levels (CTLs) of nitrogen vacancy (black horizontal bars) and substitutional O_N (red horizontal bars) in $Al_{1-x}Sc_xN$ alloys. CTLs are referenced to the valence band maximum (VBM). The bandgap (E_g) monotonically decreases with increasing Sc content (x).

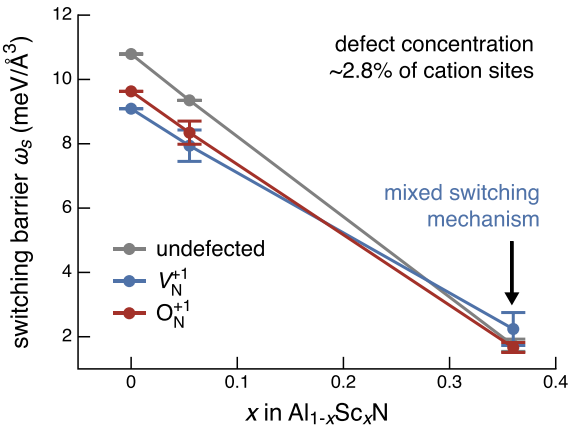

FIG. 4. Effect of dominant defects on the polarization switching barrier (ω_s) in wurtzite-type $Al_{1-x}Sc_xN$. At each Sc composition, i.e., x, ω_s is calculated at the defect sites with highest and lowest formation energies; average ω_s is plotted along with the standard deviation as the error bar. V_N^{+1} and O_N^{+1} in alloys with high Sc content exhibit mixed switching mechanisms (Fig. S11). The data for undefected $Al_{1-x}Sc_xN$ are taken from Ref. 39. The switching pathways are shown in Figs. S9–S11.

oxygen incorporation is taken into account. Here, n_e and n_h are electron and hole concentrations, respectively. The qualitative trends are similar with and without oxygen incorporation. The net carrier concentration is e^- for $n_e > n_h$ and h^+ for $n_e < n_h$. We find that, regardless of the composition, the net carrier concentration decreases under N-rich conditions. This decrease in net carrier concentration suggests that growth under N-rich conditions can effectively minimize leakage currents. Even though the net carrier concentration is predicted to be large ($>10^{12}$ cm^{-3} for $x \geq 0.250$) under N-poor conditions, the presence of very deep defect states (Fig. 3) means that the carriers will be bound and not available as free conduction carriers. Such bound carriers do not contribute to leakage current and can only be temperature activated, as is observed in pure AlN.[34]

Alloys are an ensemble of different local chemical environments, each with slightly different defect properties. Taking the example of V_N ($q = +3$), we observe variations in $\Delta E_{D,q}$ across 24 Wyckoff sites of N at each x (Fig. S8). In an attempt to correlate the variations to local environments, we plot supercell total energies as functions of the number of Sc atoms within the third nearest neighbor shell from the V_N site. We do not observe a clear trend at $x = 0.042$, 0.125, or 0.250. At $x = 0.33$, we observe a weak correlation—increasing number of Sc atoms is associated with lower V_N formation energy, which is consistent with the physical picture that local environments with more Sc are more distorted than pristine wurtzite AlN. Larger local distortions should facilitate defect formation. Future extensions of our work may also consider hydrogen defects, e.g., hydrogenated anion vacancies in AlN,[38] and cation complexes, e.g., Al vacancy complex with oxygen impurity in AlN.[22] The search for these defect complexes is computationally intensive and challenging because there is no prescribed procedure to systematically identify them.

We investigate the effects of the dominant point defects—V_N^{+1} and O_N^{+1}—on the polarization switching barrier (ω_s) of AlN and $Al_{1-x}Sc_xN$ alloys at $x = 0.055$ and 0.36. The methodology for calculating ω_s is explained in the supplementary material. We consider a defect concentration of ~2.8%, which is commensurate with the 72-atom supercell and close to the highest experimentally reported oxygen incorporation in $Al_{1-x}Sc_xN$.[32] In our recent work, we have shown that the atomic-scale polarization switching mechanism in $Al_{1-x}Sc_xN$ is composition-dependent.[39] Specifically, at low Sc compositions, e.g., $x = 0.055$, we observe collective switching, wherein the cation tetrahedra collectively undergo a transition through a hexagonal-BN-like non-polar structure and is characterized by a smooth minimum-energy pathway. In contrast, individual switching mechanism is observed at high Sc compositions, e.g., $x = 0.36$; with individual cation tetrahedra undergoing a sequential switching process through unique half-switched non-polar structures that results in complex minimum-energy pathways with ω_s typically lower than in collective mechanism.

Figure S9 shows the minimum-energy switching pathways in pristine and defected AlN (with 2.8% V_N^{+1}, O_N^{+1}). In all cases, collective switching is observed. The introduction of defects lowers ω_s relative to the undefected structure (Fig. 4). The beneficial effect of defects in lowering ω_s is surprising but consistent with design principles that we proposed in Ref. 9, namely, increased bond ionicity and softness decreases ω_s. V_N^{+1} locally softens the bonds while O_N^{+1} introduces more ionic, albeit stronger, Al–O bonds. The local structural distortions caused by the defects are qualitatively similar to distortions caused by the addition of Sc to AlN—shortening of the Al–N bonds in the basal plane and elongation of the bonds along the c axis (Fig. S12) such that the local structure is energetically "closer" to the hexagonal-BN-like non-polar phase.[40] In both cases, the structural distortions lower ω_s.

Similar behavior is observed in $Al_{1-x}Sc_xN$ alloys. At low Sc compositions ($x = 0.055$), collective switching occurs in both undefected and defected alloys. Both V_N^{+1} and O_N^{+1} (2.8%) lower ω_s (Fig. 4) and cause similar local structural distortions discussed above. However, at higher Sc composition ($x = 0.36$), the effect of the defects is less pronounced (Fig. 4). For example, the average ω_s with 2.8% O_N^{+1} is lower than the undefected alloy by < 0.1 meV/Å^3 while the average ω_s with V_N^{+1} slightly increases ω_s. As discussed earlier, an alloy is an ensemble of different local environments. At $x = 0.36$, the N site with highest (lowest) formation energy exhibits individual (collective) switching mechanism. Our previous study has shown that collective switching is

typically associated with higher ω_s.[39] As such, the average ω_s (Fig. 4) is similar to undefected $Al_{1-x}Sc_xN$.

High concentrations (>1%–2%) of defects, including unintentional impurities such as oxygen, are beyond the dilute defect limit and can impact the dielectric properties of $Al_{1-x}Sc_xN$ alloys. We quantitatively estimate their effect on E_b using Eq. (1), specifically by determining the changes in the bandgap (E_g) due to defect incorporation. Here, bandgap changes are calculated at the GGA(+U) level of theory. We found that E_g decreases upon introduction of 2.8% defects and that E_g reduction due to O_N^{+1} is less severe compared to V_N^{+1}. As a result, 2.8% O_N^{+1} reduces E_b by up to 9% while the same concentration of V_N^{+1} reduces E_b by up to 42%. The effect of O_N^{+1} on E_b is negligible ($\lesssim$3%) in $Al_{1-x}Sc_xN$ alloys at low Sc compositions.

In summary, our defect calculations reveal that nitrogen vacancies are the dominant defects in $Al_{1-x}Sc_xN$, which can be minimized by growth under N-rich conditions. Both metal and anion vacancies introduce multiple deep defect states; it is critical to minimize their concentration by growth under relatively N-rich conditions to reduce carrier recombination for optoelectronics and premature dielectric breakdown in power electronics and ferroelectrics. N-rich growth also reduces net carrier concentrations—beneficial for reducing leakage currents. High levels of unintentional oxygen incorporation are expected, with substitutional O_N present in even higher concentrations than V_N and leading to even higher leakage currents. Importantly, we find that the effect of the dominant defects on the ferroelectric properties of $Al_{1-x}Sc_xN$ is composition-dependent. Point defects, such as V_N^{+1} and O_N^{+1} (few atomic percentage concentration), favorably reduce ω_s in $Al_{1-x}Sc_xN$ at low Sc compositions but has negligible effects at high Sc compositions. It is possible that the defects may even increase ω_s at even higher Sc compositions ($x > 0.36$). Therefore, our results suggest that growing $Al_{1-x}Sc_xN$ under N-rich conditions is critical to reduce leakage current and prevent dielectric breakdown at high x while intentional introduction of nitrogen vacancy and oxygen impurity at low x may be beneficial to reduce switching barriers. In high concentrations (>2%), both defects reduce the intrinsic breakdown field but the effect of oxygen substitution on E_b reduction is less severe compared to nitrogen vacancy.

See the supplementary material for the computational methodology, phase stability, and effect of defects on bandgap and breakdown field.

This study was supported by the National Science Foundation (Grant No. DMR-2119281). The work was also partially supported by the Department of Energy Basic Energy Sciences (BES), with the additional support from the Advanced Scientific Computing Research (ASCR), under program (No. ERW6548). The research was performed using computational resources sponsored by the Department of Energy's Office of Energy Efficiency and Renewable Energy located at the NREL. The views expressed in the article do not necessarily represent the views of the DOE or the U.S. Government.

AUTHOR DECLARATIONS

Conflict of Interest

The authors have no conflicts to disclose.

Author Contributions

Cheng-Wei Lee and Naseem Ud Din contributed equally to this paper.

Cheng-Wei Lee: Data curation (equal); Investigation (equal); Writing – original draft (equal). **Naseem Ud Din:** Data curation (equal); Investigation (equal); Writing – original draft (equal). **Geoff L. Brennecka:** Project administration (equal); Writing – review & editing (equal). **Prashun Gorai:** Conceptualization (equal); Data curation (equal); Investigation (equal); Project administration (equal); Supervision (equal); Writing – review & editing (equal).

DATA AVAILABILITY

The data that support the findings of this study are available within the article and its supplementary material (Ref. 41).

REFERENCES

[1]C. E. Dreyer, A. Janotti, C. G. Van de Walle, and D. Vanderbilt, Phys. Rev. X **6**, 021038 (2016).
[2]H. Moriwake, R. Yokoi, A. Taguchi, T. Ogawa, C. A. J. Fisher, A. Kuwabara, Y. Sato, T. Shimizu, Y. Hamasaki, H. Takashima, and M. Itoh, APL Mater. **8**, 121102 (2020).
[3]S. Fichtner, N. Wolff, F. Lofink, L. Kienle, and B. Wagner, J. Appl. Phys. **125**, 114103 (2019).
[4]J. Hayden, M. D. Hossain, Y. Xiong, K. Ferri, W. Zhu, M. V. Imperatore, N. Giebink, S. Trolier-McKinstry, I. Dabo, and J.-P. Maria, Phys. Rev. Mater. **5**, 044412 (2021).
[5]K. Ferri, S. Bachu, W. Zhu, M. Imperatore, J. Hayden, N. Alem, N. Giebink, S. Trolier-McKinstry, and J.-P. Maria, J. Appl. Phys. **130**, 044101 (2021).
[6]D. Wang, P. Wang, B. Wang, and Z. Mi, Appl. Phys. Lett. **119**, 111902 (2021).
[7]D. Wang, S. Mondal, J. Liu, M. Hu, P. Wang, S. Yang, D. Wang, Y. Xiao, Y. Wu, T. Ma, and Z. Mi, Appl. Phys. Lett. **123**, 033504 (2023).
[8]Y. Dai and M. Wu, Sci. Adv. **9**, eadf8706 (2023).
[9]C.-W. Lee, N. U. Din, K. Yazawa, G. L. Brennecka, A. Zakutayev, and P. Gorai, "Emerging materials and design principles for wurtzite-type ferroelectrics," Matter **7**(4), 1644–1659 (2024).
[10]H. Mulaosmanovic, E. Chicca, M. Bertele, T. Mikolajick, and S. Slesazeck, Nanoscale **10**, 21755 (2018).
[11]K. Yazawa, J. Hayden, J.-P. Maria, W. Zhu, S. Trolier-McKinstry, A. Zakutayev, and G. L. Brennecka, Mater. Horiz. **10**, 2936 (2023).
[12]S. Calderon, J. Hayden, S. M. Baksa, W. Tzou, S. Trolier-McKinstry, I. Dabo, J.-P. Maria, and E. C. Dickey, Science **380**, 1034 (2023).
[13]T. Mikolajick, S. Slesazeck, H. Mulaosmanovic, M. H. Park, S. Fichtner, P. D. Lomenzo, M. Hoffmann, and U. Schroeder, J. Appl. Phys. **129**, 100901 (2021).
[14]K.-H. Kim, I. Karpov, R. H. Olsson, and D. Jariwala, Nat. Nanotechnol. **18**, 422 (2023).
[15]K. Yazawa, D. Drury, A. Zakutayev, and G. L. Brennecka, Appl. Phys. Lett. **118**, 162903 (2021).
[16]W. Zhu, J. Hayden, F. He, J.-I. Yang, P. Tipsawat, M. D. Hossain, J.-P. Maria, and S. Trolier-McKinstry, Appl. Phys. Lett. **119**, 062901 (2021).
[17]K. Yazawa, A. Zakutayev, and G. L. Brennecka, Appl. Phys. Lett. **121**, 042902 (2022).
[18]P. Gao, C. T. Nelson, J. R. Jokisaari, S.-H. Baek, C. W. Bark, Y. Zhang, E. Wang, D. G. Schlom, C.-B. Eom, and X. Pan, Nat. Commun. **2**, 591 (2011).
[19]A. Chouprik, D. Negrov, E. Y. Tsymbal, and A. Zenkevich, Nanoscale **13**, 11635 (2021).
[20]M. Otonicar, M. Dragomir, and T. Rojac, J. Am. Ceram. Soc. **105**, 6479 (2022).
[21]T. Mattila and R. M. Nieminen, Phys. Rev. B **54**, 16676 (1996).
[22]Q. Yan, A. Janotti, M. Scheffler, and C. G. Van de Walle, Appl. Phys. Lett. **105**, 111104 (2014).
[23]L. Gordon, J. L. Lyons, A. Janotti, and C. G. Van de Walle, Phys. Rev. B **89**, 085204 (2014).
[24]Y. Osetsky, M.-H. Du, G. Samolyuk, S. J. Zinkle, and E. Zarkadoula, Phys. Rev. Mater. **6**, 094603 (2022).

[25]J. Kataoka, S.-L. Tsai, T. Hoshii, H. Wakabayashi, K. Tsutsui, and K. Kakushima, Jpn. J. Appl. Phys., Part 1 **60**, 030907 (2021).
[26]Q. Wang, S.-X. Go, C. Liu, M. Li, Y. Zhu, L. Li, T. H. Lee, and D. K. Loke, AIP Adv. **12**, 125303 (2022).
[27]J. L. Lyons and C. G. Van de Walle, NPJ Comput. Mater. **3**, 12 (2017).
[28]J. Qu, A. Balvanz, S. Baranets, S. Bobev, and P. Gorai, Mater. Horiz. **9**, 720 (2022).
[29]N. U. Din, C.-W. Lee, K. Yazawa, W. Nemeth, R. W. Smaha, N. M. Haegel, and P. Gorai, "Defect control strategies for $Al_{1-x}Gd_xN$ alloys," chemRxiv (2023).
[30]J. L. Lyons, D. Wickramaratne, and C. G. Van de Walle, J. Appl. Phys. **129**, 111101 (2021).
[31]N. Gungor and M. Alevli, J. Vac. Sci. Technol., A **40**, 022404 (2022).
[32]J. Casamento, H. G. Xing, and D. Jena, Phys. Status Solidi (b) **257**, 1900612 (2020).
[33]M. Moram, Z. Barber, and C. Humphreys, Thin Solid Films **516**, 8569 (2008).
[34]M. Schneider, A. Bittner, and U. Schmid, Sens. Actuators, A **224**, 177 (2015).
[35]B. Saha, J. Acharya, T. D. Sands, and U. V. Waghmare, J. Appl. Phys. **107**, 033715 (2010).
[36]J.-L. Li, J. Yang, T. Wu, and S.-H. Wei, J. Mater. Chem. C **7**, 4230 (2019).
[37]C. Kim, G. Pilania, and R. Ramprasad, Chem. Mater. **28**, 1304 (2016).
[38]B. Szûcs, A. Gali, Z. Hajnal, P. Deák, and C. G. Van de Walle, Phys. Rev. B **68**, 085202 (2003).
[39]C.-W. Lee, K. Yazawa, A. Zakutayev, G. L. Brennecka, and P. Gorai, Sci. Adv. **10**, eadl0848 (2024).
[40]K. Yazawa, J. S. Mangum, P. Gorai, G. L. Brennecka, and A. Zakutayev, J. Mater. Chem. C **10**, 17557 (2022).
[41]See https://github.com/prashungorai/papers/tree/main/2024/alscn-defects-polarization-switching for "VASP input files, relaxed special quasirandom structures, relaxed defect structures, and the structures along the minimum energy pathways."